Energy Regeneration-Based Hybrid Control for Transfemoral Prosthetic Legs Using Four-Bar Mechanism

Byoung-Ho Kim
Dept. of Mechatronics Engineering
Kyungsung University
Busan, Republic of Korea
kimbh@ks.ac.kr

Hanz Richter
Dept. of Mechanical Engineering
Cleveland State University
Cleveland, USA
h.richter@csuohio.edu

***Abstract*—This paper presents an energy regeneration-based hybrid control method for transfemoral prosthetic legs using a four-bar linkage mechanism. To do that, we consider a model of transfemoral prosthetic leg with three-degrees of freedom that employs a knee mechanism using a four-bar linkage mechanism. We also focus on suggesting a practical strategy for effective implementation rather than a complex algorithm. In this point of view, we devise a hybrid controller for the prosthetic leg. Actually, the motions of the hip mechanism of the leg are controlled by a PID control method and the knee joint is controlled by an impedance control method. We also consider an electrical energy regeneration module for effective energy utilization. Through an exemplary walk simulation, we show the availability of the hybrid controller for such a transfemoral prosthetic leg and also address the advantages of using such a four-bar mechanism and an energy regeneration module for effective driving the knee joint. It is finally concluded that the proposed hybrid controller can be applied for effective control of transfemoral prosthetic legs using such a four-bar mechanism.**

***Index Terms*—transfemoral prosthetic leg, four-bar linkage mechanism, energy regeneration, hybrid control**

I. Introduction

It is well-known that the objective of research on transfemoral prosthesis is to replace a leg missing above the knee as an artificial limb. This effort is very helpful for amputees to regain normal movement. Initially, many passive prostheses were developed and used by transfemoral amputees [1]. In fact, these passive prostheses put a lot of strain on their hip joints because those mechanisms are somewhat heavy and have no power to drive any joint. Thus, transfemoral amputees walking with these passive prostheses consume much more energy during walking compared to healthy people [2]. Especially, the hip joints with these passive prostheses have several times more burden than the normal hip joints [3]. This burden can be alleviated by using a powered prosthesis [4].

Actually, there are many challenges in developing the powered transfemoral prosthesis, as shown in Fig. 1, in terms of mechanical design, effective energy utilization and control, biomimetic motion planning, and so on. Recently, in order to develop an effective powered transfemoral prosthesis, many studies have been actively conducted [5] - [8]. Sup, *et. al.* presented a remarkable consideration on design of powered transfemoral prostheses [5]. Actually, related to driving the knee joint mechanism, they considered a slider-crank mechanism and a pneumatically actuated powered-tethered device. An embedded control system has been specified for effective control of a prosthetic leg mechanism [7]. A user-oriented transfemoral prosthesis approach is also remarkable for effective walking because it considers a whole-body awareness [8]. And a remote controller using a high-speed CAN Bus has been proposed for a transfemoral prosthesis [9]. However, they did not show the performance of their prosthesis in terms of a leg. In fact, although a prosthesis is an independent part, once it is attached to a person, it is no longer an independent part. That is, the control performance of the prosthesis could be affected by the style of the hip movement of an amputee. Therefore, it is necessary to consider the overall dynamic characteristics of the leg with a prosthesis to achieve more comfortable walk performance.

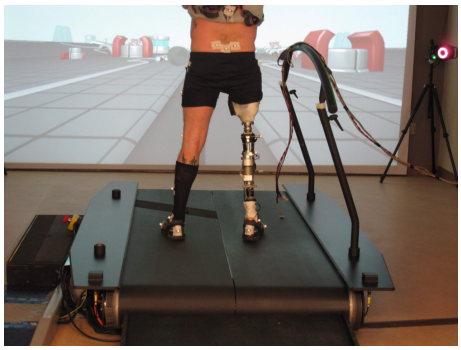

Fig. 1. A powered transfemoral prosthetic leg using a four-bar linkage mechanism (Copyright: Cleveland FES Center, Cleveland, USA)

In terms of effective energy utilization, a remarkable framework of energy regeneration has been presented [10] and an optimal control method has been proposed for effective control of transfemoral prostheses using such an energy regeneration [11]. They showed the feasibility of their optimal control approach for a proper combination of control performance and energy recycling. Nevertheless, more simplification of the

978-1-5090-6683-4/18/$31.00 ©2018 IEEE

overall control algorithm remains a challenge.

The objective of this paper is to present an energy regeneration-based hybrid control method for effective control of transfemoral prosthetic legs using a four-bar linkage mechanism. Our focus is to devise a practical strategy for effective implementation rather than a complex algorithm. The features of using a four-bar mechanism and an energy regeneration module are also discussed in terms of effective energy utilization. It is finally shown that our approach is available for effective control of transfemoral prosthetic legs using such a four-bar mechanism.

II. Modeling and Control of Transfemoral Prosthetic Leg

This section reveals a typical model of transfemoral prosthetic leg mechanisms and describes its dynamic relationship.

Fig. 1 shows a situation that an amputee is testing the performance of a powered transfemoral prosthetic leg using a four-bar linkage mechanism through walking on a treadmill. In order to deal with the control problem of such a transfemoral prosthetic leg, the human walk has been simplified as a bipedal robot walk as shown in Fig. 2, where the prosthetic leg is only considered for the control problem.

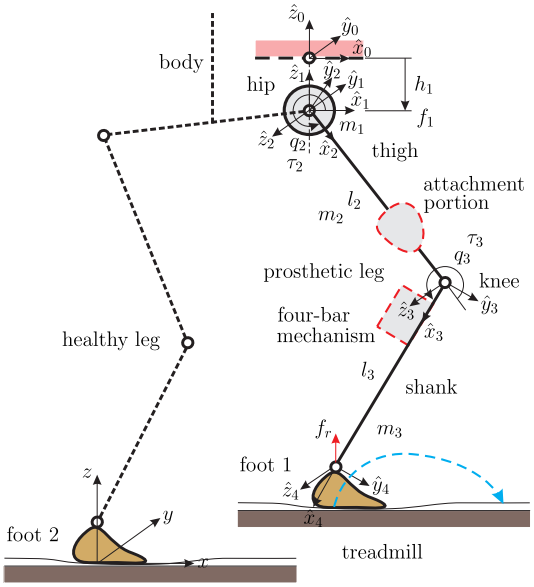

Fig. 2. A bipedal robot walk

The dynamic equation of the prosthetic leg in Fig. 2 is generally described by the following form at the joint space [12]:

$$\boldsymbol{M}(q)\ddot{q} + \boldsymbol{B}(q)[\dot{q}\dot{q}] + \boldsymbol{C}(q)[(\dot{q})^2] + g(q) + u_L = u \qquad (1)$$

where q, $\dot{q}$ and $\ddot{q}$ are the $n \times 1$ vectors of joint angular position, velocity and acceleration, respectively. u is the $n \times 1$ vector of generalized force and torque supplied by actuators. $\boldsymbol{M}(q)$ is a $n \times n$ symmetric positive definite inertia matrix. $\boldsymbol{B}(q)[\dot{q}\dot{q}]$ and $\boldsymbol{C}(q)[(\dot{q})^2]$ are $n \times 1$ vectors representing the Coriolis and centrifugal terms. $g(q)$ is the $n \times 1$ vector of gravity. u_L represents the generalized force and torque vector that supports the external force activated in the leg.

The generalized force and torque vector in (1) is given by

$$u = \begin{bmatrix} f_1 & \tau_2 & \tau_3 \end{bmatrix}^T \qquad (2)$$

where f_1 represents the force for the vertical motion of the overall hip joint. τ_2 and τ_3 represent the torques for the rotational motion of the hip joint and the knee joint, respectively. In our consideration, the vertical force and rotational torque of the hip joint are supplied by using an external power source. But the knee joint torque is made by an embedded self-power module as shown in Fig. 3.

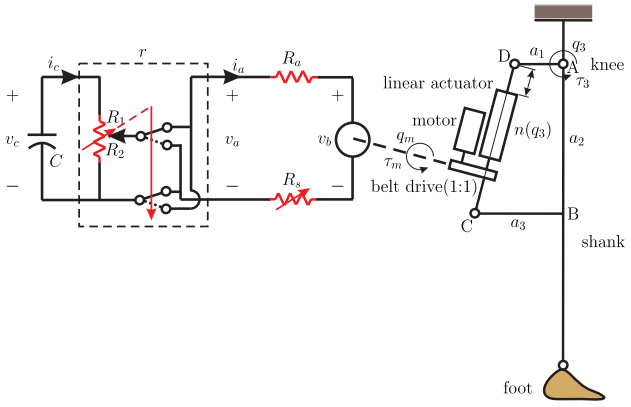

Fig. 3. A prosthetic knee system using a four-bar mechanism and a self-power module

In fact, the knee system shown in Fig. 3 utilizes a kind of four-bar linkage mechanism driven by an electric motor. This mechanism is a typical electro-mechanical system and very useful in terms of torque utilization. Actually, the torque for driving the knee joint can be expressed as follows.

$$\tau_3 = n(q_3)\tau_m \qquad (3)$$

where the torque ratio $n(q_3)$ relating the drive motor space to the knee joint space can be driven by

$$n(q_3) = \frac{a_1 a_4 \sin(q_3 + q_{DAC0})}{\eta\sqrt{(a_1)^2 + (a_4)^2 - 2a_1 a_4 \cos(q_3 + q_{DAC0})}} \qquad (4)$$

here a_1 is the length of the link DA in the four-bar mechanism and a_4 represents the length of the line $\overline{AC}$. η denotes the ratio relating the rotation angle of the linear actuator to its linear movement, and q_{DAC0} is the angle A of the virtual triangle consisting of DAC at the initial configuration. Note that the joint motion of the linear actuator is the same as that of the drive motor because the belt drive ratio is 1:1.

Based on the motor relationship and the electric network, the torque of the drive motor τ_m can be determined by

$$\tau_m = \frac{1}{R} k_m (r v_c - \tau_{bemf}) \qquad (5)$$

where k_m represents the motor constant, and the resistance of the network R is determined by the sum of the resistance of the armature R_a and the additional resistance R_s. The role of the parameter r is to divide the voltage of the capacitor v_c,

and it can be adjusted to a value between 1 and -1. The back electro-mechanical force τ_{bemf} can be expressed by

$$\tau_{bemf} = \frac{1}{R}(k_m)^2 n(q_{3a})\dot{q}_{3a} \tag{6}$$

where $\dot{q}_{3a}$ represents the actual angular velocity of the knee joint.

Then, we propose a hybrid controller for the operation of the prosthetic leg as follows. It is actually made by combining the conventional PID(Proportional, Integral, and Derivative) controller and an impedance controller. Firstly, the vertical and rotational motions of the hip are controlled by the PID control law as follows.

$$f_1 = k_{p1}\delta h_1 + k_{d1}\delta v_1 + k_{i1}\sum \delta h_1 \tag{7}$$

$$\tau_2 = k_{p2}\delta q_2 + k_{d2}\delta w_2 + k_{i2}\sum \delta q_2 \tag{8}$$

where k_{pj}, k_{dj}, and k_{ij} represent the proportional, derivative, and integral gains for the jth motion. The parameters of δh_1 and δv_1 are the position and velocity errors of the vertical movement of the hip, respectively. δq_2 and δw_2 represent the rotational angular position and velocity errors of the hip joint.

Secondly, the motion of the knee joint is controlled by the following impedance control law:

$$\tau_m = k_{pm}\delta q_m + k_{dm}\dot{q}_{ma} \tag{9}$$

where δq_m and $\dot{q}_{ma}$ are the position error and the actual angular velocity of the drive motor, respectively, and k_{pm} and k_{dm} represent the proportional and damping gains for the actuator. The actual angle and angular velocity of the drive motor can be determined by

$$q_{ma} = \frac{\sqrt{(a_1)^2 + (a_4)^2 - 2a_1a_4\cos(q_{3a} + q_{DAC0})} - l_{CD0}}{\eta} \tag{10}$$

$$\dot{q}_{ma} = n(q_{3a})\dot{q}_{3a} \tag{11}$$

here l_{CD0} and q_{3a} represent the length of the line $\overline{CD}$ at the initial configuration and the actual angle of the knee joint, respectively.

Since the knee joint is actually driven by using the embedded self-power module, the torque of the knee joint can be made by controlling the parameter r which is determined by using (3), (5) and (9) as follows.

$$r = \frac{R}{k_m v_c}(\tau_m - \tau_{bemf}). \tag{12}$$

Simultaneously, the real-time voltage of the capacitor considering discharge and recharge can be determined by

$$v_c(t + dt) = v_c(t) - \frac{1}{C}i_c(t)dt \tag{13}$$

where C and $i_c(t)$ represent the capacitance and current parameters of the capacitor, respectively, and dt is the sampling time. Practically, the voltage of the capacitor can be increased when the current is negative, and this activity is helpful for a long time walk after attaching the prosthetic leg.

As a result, using (3) and (7)∼(13), we can control the transfemoral prosthetic leg shown in Fig. 2. The availability of the specified hybrid control approach is shown in the next section.

III. Walk Simulation and Discussion

To demonstrate the usefulness of the proposed hybrid controller, this section provides an exemplary walk simulation using the transfemoral prosthetic leg in Fig. 2 and interesting discussions.

For effective simulation, we performed a repetitive stepping walk of the transfemoral prosthetic leg on a treadmill as shown in Fig. 2. By observing the walk style of a human [13]- [15], the trajectories set for the walking task were planned as Fig. 4. Especially, note that the y-directional motion of the leg has been constrained on 0.2 m. The z-directional trajectories of the hip joint and the foot can be described by combining a cubic and triangular functions, but they have been omitted because of the limited space.

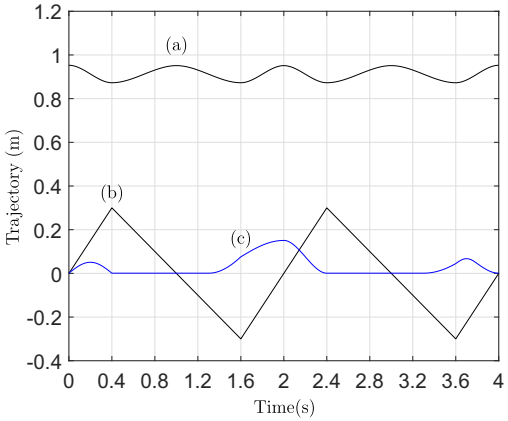

Fig. 4. Trajectories set for the walking task: (a) z-directional movement of the hip, (b) x-directional movement of the foot, and (c) z-directional movement of the foot.

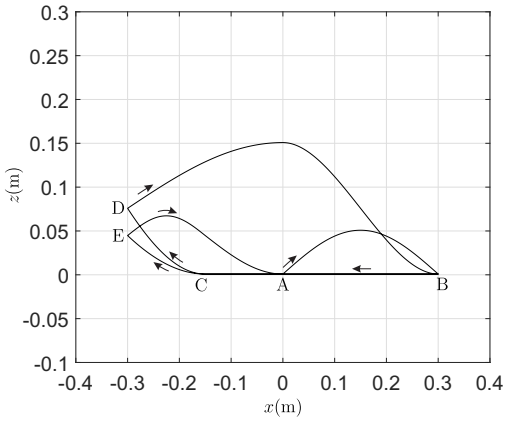

Fig. 5. Trajectory of the foot in the xz-planar space for the prosthetic walk

The trajectory of the foot in the xz-planar space for the walking task can be shown as Fig. 5. It forms a kind of iterative loop. The foot trajectory given in this study proceeds actually in the order of A→B→C→D→B→C→E→A, where the point A is the starting or end position. The stage from A to B is for

a ready step to start the recursive walk, and the stage from E to A is to finish the recursive walk. The stage from C to D, or from C to E, means a lifting operation of the heel of the foot to enter the swing phase. Such a repetitive walking can be performed by following the closed loop B→C→D.

Our simulation has been performed under the condition that the initial posture of the leg is an upright posture, and each part should follow the trajectory assigned in Fig. 4. The corresponding system parameters for this simulation were specified in Table I. Especially, the reaction force at the foot was calculated by using stiffness relationship, where the stiffness of the treadmill was set to 37000 N/m. The friction coefficient of the treadmill was set to 0.25, and the initial voltage of the self-power module was assigned as 20 V. The gain parameters for the hybrid controller described in Section II were assigned as Table II. The sampling time for the control of each walk was set to 5 ms.

TABLE I
SYSTEM PARAMETERS FOR THE WALK SIMULATION

Parameter	Value	Unit
length of thigh (l_2)	0.425	m
length of shank (l_3)	0.527	m
mass of hip (m_1)	40.6	kg
mass of thigh (m_2)	8.57	kg
mass of shank (m_3)	4.29	kg
DC motor constant (k_m)	0.06	Nm/A
armature resistance (R)	0.1	Ω
setting resistance(R_s)	0	Ω
capacitance (C)	500	F

TABLE II
GAIN PARAMETERS FOR THE HYBRID CONTROLLER

j	PID controller			Impedance Controller	
	k_{pj}	k_{dj}	k_{ij}	k_{pj}	k_{dj}
1	68500	3425	1712.5	-	-
2	400	1.4	0.2	-	-
m	-	-	-	0.25	0.0008

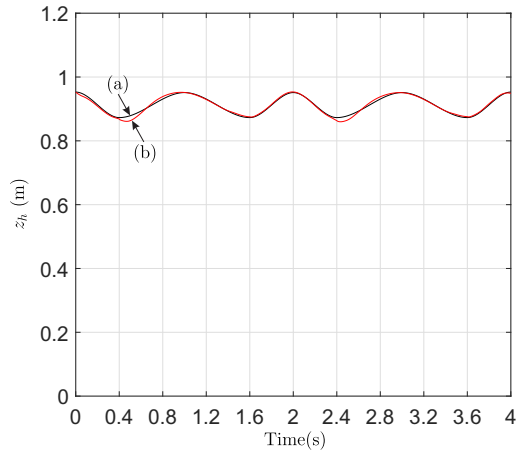

Fig. 6. Trajectory following result for the vertical motion of the hip: (a) desired trajectory and (b) actual trajectory.

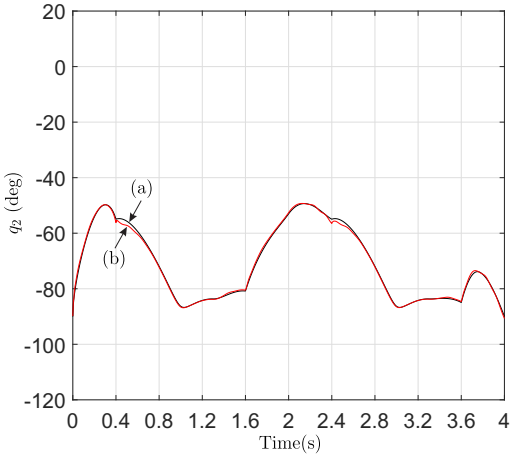

Fig. 7. Trajectory following result for the rotational motion of the hip joint: (a) desired trajectory and (b) actual trajectory.

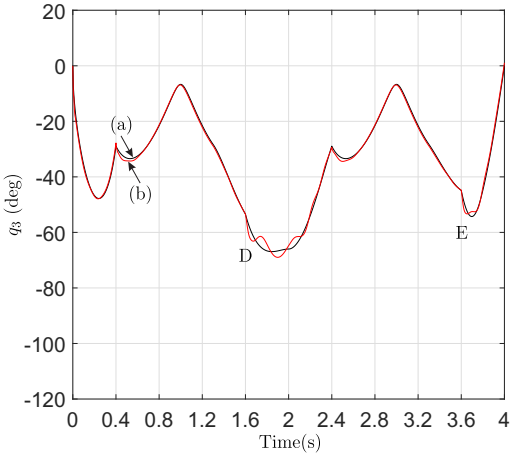

Fig. 8. Trajectory following result for the rotational motion of the knee joint: (a) desired trajectory and (b) actual trajectory.

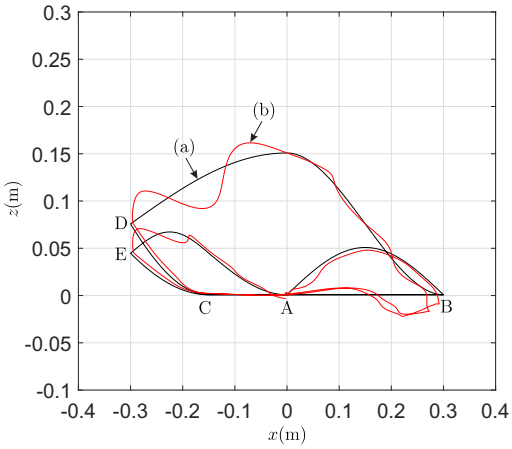

Fig. 9. Trajectory following result of the foot in the xz-planar space: (a) desired trajectory and (b) actual trajectory.

Through this simulation, we confirmed the desired and actual trajectories for the vertical motion of the hip and the rotational motion of the hip joint, and they have been shown in Fig. 6 and Fig. 7. Fig. 8 shows the desired and actual angular trajectories of the knee joint for the walk. From these

figures, it can be seen that the actual trajectories follow their desired trajectories satisfactorily. Also, the resultant trajectory following result of the foot in the xz-planar space has been plotted in Fig. 9. Specifically, the actual trajectory deviates significantly from the desired trajectory at points B, D, and E in Fig. 9, but after those points, the actual trajectory has been properly controlled. This phenomenon can be seen as the effect of the reaction force shown in Fig. 10, which is actually caused from landing of the foot on the walk surface or take off. From Fig. 8, we can also recognize that the motion of the knee joint can be affected by the reaction force.

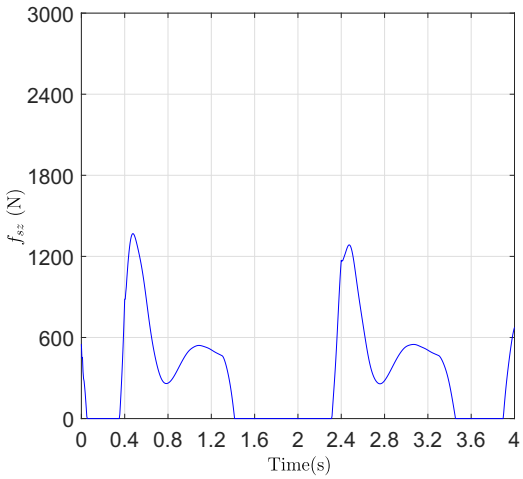

Fig. 10. Reaction force to the z-direction

Also, we confirmed the desired and actual force profiles for the vertical motion of the hip and the desired and actual torques for the rotational motion of the hip joint as shown in Fig. 11 and Fig. 12, respectively. In particular, we can see that a relatively large torque value appears when the foot touches down on the walk surface repeatedly at 0.4 s and 2.4 s.

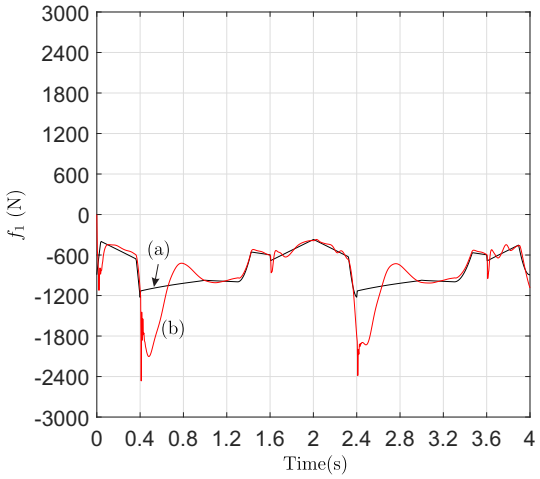

Fig. 11. Forces supporting the vertical motion of the hip: (a) desired force and (b) actual force.

Fig. 13 shows the torque performance of the drive motor for the actuation of the knee joint, where the torque range is confirmed to be within $|20|$ Nm. It is very reasonable range for

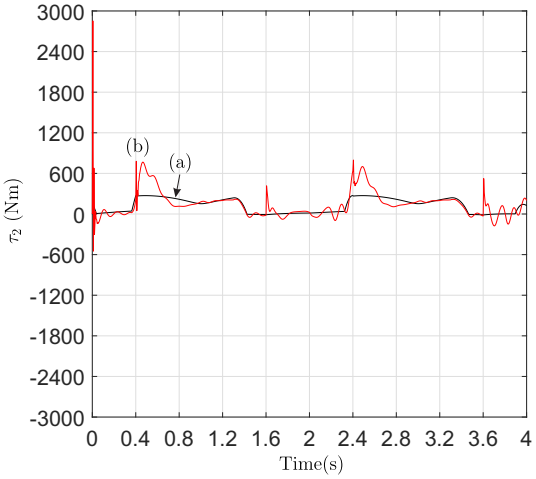

Fig. 12. Torques supporting the rotational motion of the hip joint: (a) desired torque and (b) actual torque.

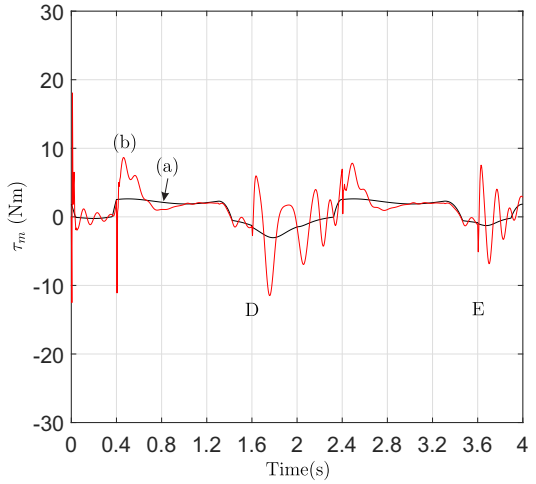

Fig. 13. Torques of the drive motor for the actuation of the knee joint: (a) desired torque and (b) actual torque.

practical implementation. This advantage could be obtained by employing the four-bar mechanism shown in Fig. 3 to drive the knee joint. Actually, the four-bar mechanism enables us to utilize the torque ratio in (3) and (11), and the ratio in this study has been illustrated in Fig. 14. Note that the torque ratio is not constant and depends on the motion of the knee joint. Also, we can confirm that a large change of torque at points D and E in Fig. 13 reliably support the response shown in Fig. 8.

In addition, the control parameter for effective supplying the embedded self-power into the drive motor and the voltage of the capacitor which changes in real time have been shown in Fig. 15 and Fig. 16, respectively. Actually, we can confirm that the initial voltage of the capacitor is 20 V, and it is gradually reduced by being used in real time for the knee joint motion. This gentle pattern is due to the fact that some voltage is recharged in the course of the knee motion. Recently, a performance test on a knee controller has been performed [16]. In fact, this effort to improve the performance of such energy recharging is very important to increase the time of

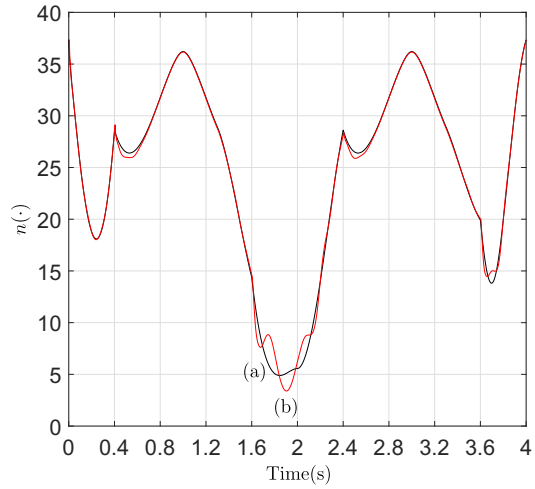

Fig. 14. Torques ratios relating the drive motor space to the knee joint space: (a) the ratio determined by the desired angular trajectory of the knee joint q_{3d} and (b) the ratio by the actual angular trajectory q_{3a}.

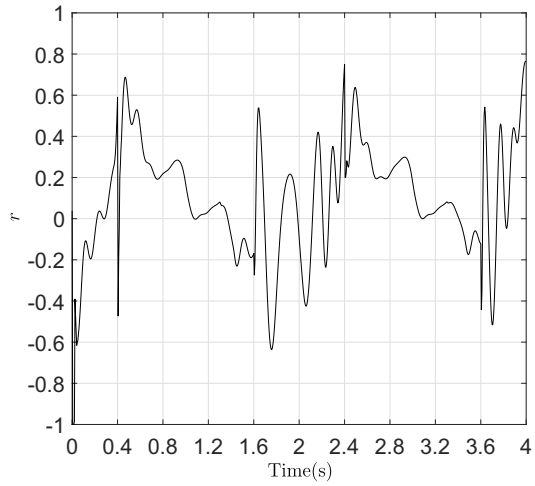

Fig. 15. Control parameter r's profile

use of the prosthetic leg. So, additional research on this effort is required in future.

As a result, we can remark that the proposed hybrid control method is useful for a transfemoral prosthetic leg using a four-bar mechanism through an exemplary walk simulation. It is also remarked that such a four-bar mechanism and the embedded self-power module are available for effective driving the knee joint.

IV. Concluding Remarks

In this paper, we presented an energy regeneration-based hybrid control method for transfemoral prosthetic legs using a four-bar linkage mechanism and showed its usefulness through an exemplary walk simulation. The proposed hybrid controller is actually not complex and very useful for practical implementation. We also addressed the advantages of using such a four-bar mechanism and an energy regeneration module for effective driving the knee joint. As a result, it is finally concluded that the proposed hybrid controller can be used for effective control of transfemoral prosthetic legs using a four-bar mechanism. One of interesting future works will be the study on effective energy recharging by considering more practical walking strategy.

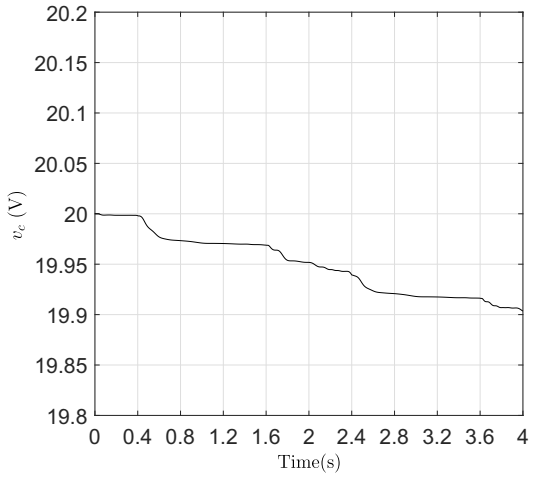

Fig. 16. Voltage profile of the capacitor

References

[1] S. B. O'Sullivan and T. J. Schmitz, Physical Rehabilitation, 5th ed., F.A. Davis Company, 2007.

[2] R. Waters, J. Perry, D. Antonelli, and H. Hislop, "Energy cost of walking amputees: the influence of level of amputation," Jour. of Bone and Joint Surgery, vol. 58A, pp. 42–46, 1976.

[3] D. A. Winter, The Biomechanics and Motor Control of Human Gait: Normal, Elderly and Pathological, 2nd ed., Waterloo, ON, University of Waterloo Press, 1991.

[4] G. K. Klute, J. Czerniecki, and B. Hannaford, "Development of powered prosthetic lower limb," Proc. of the 1st National Meeting, Veterans Affairs Rehabilitation Research and Development Service, 1998.

[5] F. Sup, A. Bohara, and M. Goldfarb, "Design and contol of a powered transfemoral prosthesis," The International Jour. of Robotics Research, vol. 27, no. 2, pp. 263–273, February 2008.

[6] S. K. Au and H. M. Herr, "Powered ankle-foot prosthesis," IEEE Robotics & Automation Magazine, vol. 15, no. 3, pp. 52–59, 2008.

[7] B. E. Lawson, J. E. Mitchell, D. Truex, A. Shultz, E. Ledoux, and M. Goldfarb, "A robotic leg prosthesis-design, control, and implementation," IEEE Robotics & Automation Magazine, pp. 70–81, December 2014.

[8] L. Ambrozic, M. Gorsic, J. Geeroms, L. Flynn, R. M. Lova, R. Kamnik, M. Munih, and N. Vitiello, "Cyberlegs-a user-oriented robotic transfemoral prosthesis with whole-body awareness control," IEEE Robotics & Automation Magazine, pp. 82–93, December 2014.

[9] T. Lenzi, L. J. Hargrove, and J. W. Sensinger, "Speed-adaptation mechanism-robotic prostheses can actively regulate joint torque," IEEE Robotics & Automation Magazine, pp. 94–107, December 2014.

[10] H. Richter, "A framework for control of robots with energy regeneration," ASME Jour. of Dynamic Systems, Measurement, and Control, vol. 137, no. 9, pp. 091004-1–11, September 2015.

[11] G. Khademi, H. Mohammadi, H. Richter, and D. Simon, "Optimal mixed tracking/impedance control with application to transfemoral prostheses with energy regeneration," IEEE Trans. on Biomedical Engineering, vol. 65, no. 4, pp. 894–910, April 2018.

[12] J. J. Craig, Introduction to robotics mechanics and control, 3rd. ed. Prentice Hall, 2004.

[13] J. Perry, Gait Analysis, SLACK, INC., 1992.

[14] C. C. Norkin and P. K. Levangie, Joint Structure & Function, F. A. Davis, Co., 1992.

[15] A. D. Kuo, "Choosing your steps carefully," IEEE Robotics & Automation Magazine, pp. 18–29, June 2007.

[16] P. Khalaf, H. Warner, E. Hardin, H. Richter, and D. Simon, "Development and experimental validation of an energy regenerative prosthetic knee controller and prototype," Pro. of the ASME 2018 Dynamic Systems and Control Conference, Accepted, 2018.